Solar Energy Materials & Solar Cells 125 (2014) 310–317

Contents lists available at ScienceDirect

Solar Energy Materials & Solar Cells

journal homepage: www.elsevier.com/locate/solmat

Numerical optimization of multilayer electrodes without indium for use in organic solar cells

Adrien Bou [a,d], Philippe Torchio [a,*], Sylvain Vedraine [a], Damien Barakel [a], Bruno Lucas [b], Jean-Christian Bernède [c], Pierre-Yves Thoulon [d], Marc Ricci [d]

[a] Aix-Marseille University, Institut Matériaux Microélectronique Nanosciences de Provence-IM2NP, CNRS-UMR 7334, Domaine Universitaire de Saint-Jérôme, Service 231, 13 397 Marseille Cedex 20, France
[b] Limoges University, XLIM Institute, CNRS-UMR 7252, Université de Limoges, 123 avenue Albert Thomas, 87 060 Limoges, France
[c] LUNAM University, MOLTECH-Anjou, CNRS-UMR 6200, UFR Sciences, 2 Rue de la Houssinière, 44 322 Nantes, France
[d] CROSSLUX, Immeuble CCE, Avenue Georges Vacher, ZI Rousset Peynier, 13 106 Rousset Cedex, France

ARTICLE INFO

Available online 13 February 2014

Keywords:
Free-ITO electrode
Oxide/metal/oxide
Organic solar cell
Optical optimization
TMM
Intrinsic absorption efficiency

ABSTRACT

A numerical process is developed on a Transfer-Matrix Method (TMM) to calculate the optical properties of multilayers involved in thin film solar cells. Using the bulk complex refractive indices in a considered spectral range for each material allows us to calculate the transmittance of the whole structure and the intrinsic absorption inside the sole active layer. An optical optimization of oxide|metal|oxide trilayer electrode in the air and with a (poly-3-hexylthiophene):[6,6]-phenyl-C_{61}-butyric acid methyl ester (P3HT:PCBM) bulk heterojunction based organic solar cell is performed. The ZnO|Ag|ZnO structure is specifically studied in order to avoid the use of indium in such photovoltaic components.

1. Introduction

Organic Solar Cells (OSCs) are considered as a very promising way for the next generation photovoltaics. For about ten years, efficiency has moved up from a few percent to 11.1% [1–3]. New applications result from OSC's ability to be at the same time low-cost, flexible and semi-transparent. Indium Tin Oxide (ITO) is one of the most used Transparent Conductive Oxides (TCOs) as OSC's transparent electrode. Unfortunately, indium is rare on earth and could become very expensive if its consumption continues to grow (Liquid Crystal Display, CIGS solar cells, ITO, etc.). Moreover, the sheet resistance (R_S) of ITO can significantly increase with cyclic bending beyond low bending radius (< 10 mm) [4,5]. Cracks occur affecting the quality of the OSC.

Alternatives [6,7] to this material are currently developed such as multilayer electrodes [8]. They usually consist in an oxide|metal|oxide (OMO) trilayer. The oxide layers can sometimes be replaced by sulfide layers. The strength of such arrangement is to be able to provide a high transmittance and a high conductivity. The transparency of the structure can be higher than those for a single thin metal layer due to a strong influence of optical interferences in the trilayer stack. Another advantage is to be more resistant to cyclic bending [4,9] compared to ITO. The OMO electrode also limits the exposition of the bulk heterojunction to humidity thanks to the thin-metal layer [10–12]. This trilayer can also be referenced TCO|metal|TCO electrodes. The basic points to select materials constituting the trilayer are the following: oxides need to have a high refractive index and a low extinction coefficient at visible wavelengths; metal should have a high conductivity, with as low as possible extinction coefficient values, even at very low thicknesses (around 10 nm); oxide of the active layer side has to show relevant carrier-collection properties to be suitable in OSC and be able to avoid the adjunction of a buffer layer.

The choice of both oxides – or even sulfides – can be done among a wide range of materials such as In_2O_3, SnO_2, ZnO, ITO, MoO_3, Al_2O_3, WO_3, TiO_2, V_2O_5, ZnS, Zinc Tin Oxide (ZTO), Aluminum Zinc Oxide (AZO), Fluorine Tin Oxide (FTO), Gallium Zinc Oxide (GZO), etc. The oxides in the trilayer may or may not be the same. Many possibilities without indium can then be studied. The metal layer may be selected from Ag, Au, Cu, Al, Mo, etc. Such a variety of the OMO structure design is illustrated in Table 1 which presents a recent overview from literatures [13–19] at the state-of-the-art [13–31]. This Table provides the transmittance T_{550} at a wavelength of 550 nm, the sheet resistance R_S and the figure of merit Φ_T of the manufactured electrodes regarding several kinds of OMO trilayers made with several deposition methods. The figure of merit, proposed by Haake [32], for transparent conductors is given by

$$\phi_T = \frac{T^{10}}{R_s} \tag{1}$$

The conductivity of the OMO multilayer is mainly controlled by the thickness of the metal film. Above a critical value which ranges generally between 5 and 15 nm, the resistivity drops down drastically [19,33]. This limit value depends on the metal, but also on the underlying oxide and on the employed deposition method and speed

* Corresponding author.
E-mail address: philippe.torchio@univ-amu.fr (P. Torchio).

0927-0248/$ - see front matter © 2014 Elsevier B.V. All rights reserved.
http://dx.doi.org/10.1016/j.solmat.2013.12.026

Table 1
Recent overview of some TCO|metal|TCO electrodes with their thicknesses, their transmittance at a wavelength of 550 nm, their sheet resistance and their figure of merit (see Eq. (1))/DC MS (Direct Current Magnetron Sputtering) – IBS (Ion Beam Sputtering) – JEE (Joule Effect Evaporation) – RS (Reactive Sputtering) – RF MS (Radio Frequency Magnetron Sputtering).

Structure	Deposition Method	T_{550} (%)	R_S (Ω/□)	Φ_T ($\times 10^{-3}\,\Omega^{-1}$)	Year and reference
Glass|GZO(40)|Ag(12)|GZO(40)	DC MS	87	6	41	2009 [13]
Glass|AZO(40)|Ag(12)|GZO(40)	DC MS	82	7	20	2009 [13]
Glass|ZnO(35)|Ag(10)|ZnO(20)	IBS	80	6.5	17	2012 [14]
Glass|MoO_3(20)|Ag(11)|MoO_3(35)	JEE	76[a]	4	18	2013 [15]
Glass|ZnO(25)|Au(8)|ZnO(25)	RS	–	–	58	2012 [16]
PET|ITO(20)|Ag(7)|ITO(20)	RS	–	–	29	2012 [16]
Glass|$CuAlO_2$(40)|Ag(8)|$CuAlO_2$(40)	RF MS	89	9.7	32	2010 [17]
Glass|ZTO(20)|Ag(8)|ZTO(39)	RF MS	84	8.8	20	2011 [18]
Glass|AZO(30)|Mo(15)|AZO(30)	RF MS	80	12.0	9	2013 [19]

[a] Value of the averaged transmission in the [400–700] nm spectral band.

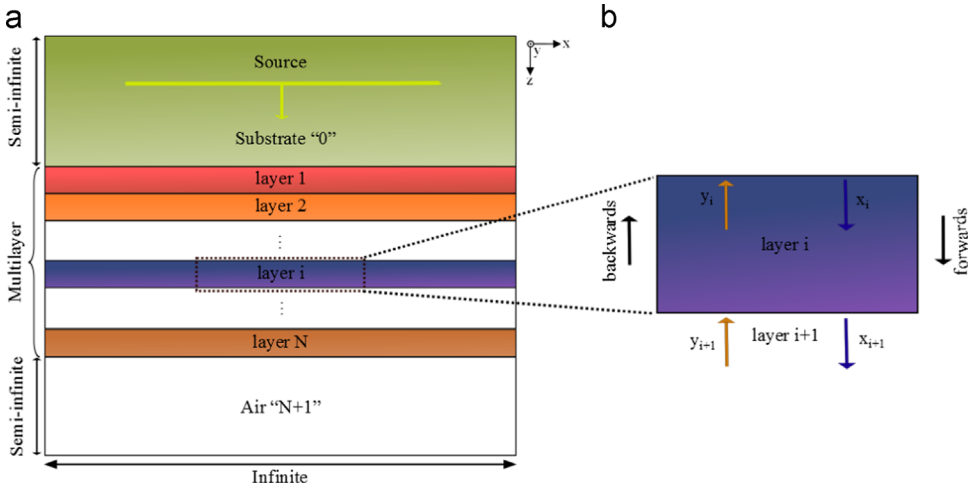

Fig. 1. (a) Design of the modeled multilayer stack and (b) schematics of layer *i*. At the top, x_i is the amplitude of the wave – at the interface – going forward into layer *i* and y_i is the amplitude of the wave going backward from layer *i*. At the bottom, x_{i+1} is the amplitude of the wave going forward out of layer *i*, and y_{i+1} is the amplitude of the wave going backward from the next layer.

[15]. The thicknesses of each layer of the OMO electrode can be optimized to reach the highest transmittance in the desired spectrum [34]. The considered spectral band depends on the active layer's absorption spectral range of the OSC which is further carried out on the transparent electrode. The metal layer morphology is also a key point [35] to successfully embed the OMO transparent electrode in OSC. A non-uniform, island-like morphology can increase R_S due to the lack of connectivity of the metal islands. This morphology can also induce optical scattering and surface plasmon resonance (SPR) that lead to increased photon absorption [4,35–38].

This study presents an optical numerical optimization method of such a multilayer electrode in the air and embedded in an OSC based on P3HT:PCBM (with a volume ratio of 1:1) as active layer. By using our numerical method, it is possible to improve the understanding of the optical behavior of such a trilayer anode, and to reach its optimal use for OSC or for other fields in optoelectronics.

2. Numerical method

2.1. Transfer-Matrix Method

The calculation is done by a Transfer-Matrix Method (TMM) from Abeles [39] and described by Dyakov et al. [40]. This method is a first approach, which assumes that the layers of a multilayer stack are planar, massive and homogeneous, that light comes from a semi-infinite substrate – made of glass or poly(ethylene terephthalate) (PET) – at normal incidence and that the structure is surrounded by air.

The design of the stack considered in our study is defined in Fig. 1(a), where *N* layers are placed between the substrate "0" and the air "$N+1$". For each layer, the dispersion of the bulk complex refractive indices is used as data input in the suitable spectral range. Our method allows us to calculate the optical properties (reflectance, transmittance, and absorptance) for one or many layers.

The refraction is described by the Snell–Descartes laws and takes into account the incidence angle at each interface [40]. In our study, the calculation is performed at normal incidence $\theta_i = 0°$. The $\boldsymbol{k}_{z,i}$ *z*-component of the complex wave vector in each *i* layer

$$\boldsymbol{k}_{z,i} = \frac{2\pi}{\lambda}\tilde{n}_i(\lambda)\cos(\theta_i) = \frac{2\pi}{\lambda}\tilde{n}_i(\lambda) \tag{2}$$

with λ the wavelength of the incident light and $\tilde{n}_i$ the complex refractive index of the *i* layer material which is defined by

$$\tilde{n}_i(\lambda) = n_i(\lambda) + j\kappa_i(\lambda) \tag{3}$$

with $\left\{ n_i(\lambda) = \frac{c}{v_i} \right.$ the real refractive index, c the vacuum speed of light and v_i the phase speed of light in the i layer$\kappa_i(\lambda)$ the imaginary extinction coefficient.